

Supplementary Information

Hot carrier dynamics in metalated porphyrin-naphthalimide thin films

Md Soif Ahmed,^a Sudhanshu Kumar Nayak,^a Botta Bhavani,^{b,c} Dipanjan Banerjee,^d Seelam Prasnathkumar,^{b,c} Lingamallu Giribabu,^{b,c} Venugopal Rao Soma,^d Sai Santosh Kumar Raavi^{a,e,*}

^a Ultrafast Photophysics and Photonics Laboratory, Department of Physics, Indian Institute of Technology Hyderabad, Kandi 502285, Telangana, India

^b Polymers & Functional Materials Division, CSIR-Indian Institute of Chemical Technology, Tarnaka, Hyderabad-500007, India

^c Academy of Scientific and Innovative Research (AcSIR), Ghaziabad- 201002, India

^d Advanced Centre of Research in High Energy Materials (ACRHEM), DRDO Industry Academia – Centre of Excellence (DIA-COE), University of Hyderabad, Hyderabad 500046, Telangana, India

^e Department of Climate Change, Indian Institute of Technology Hyderabad, Kandi 502285, Telangana, India

**Corresponding author's e-mail address: sskraavi@phy.iith.ac.in*

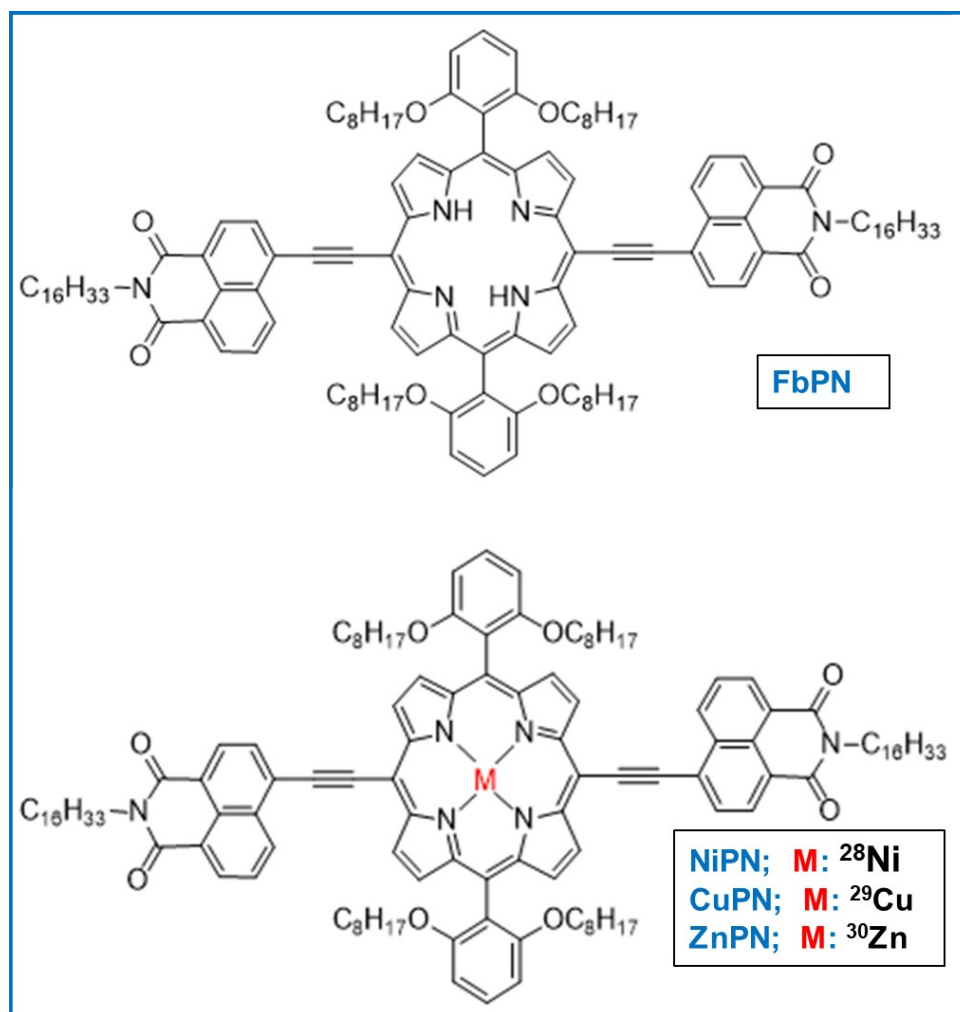


Fig. S1 Molecular structures of free base and transition metalated porphyrin-naphthalimide (PN) systems; FbPN is represented for the free base, NiPN, CuPN, and ZnPN are represented for Ni(II), Cu(II) and Zn (II) metalated derivatives respectively.

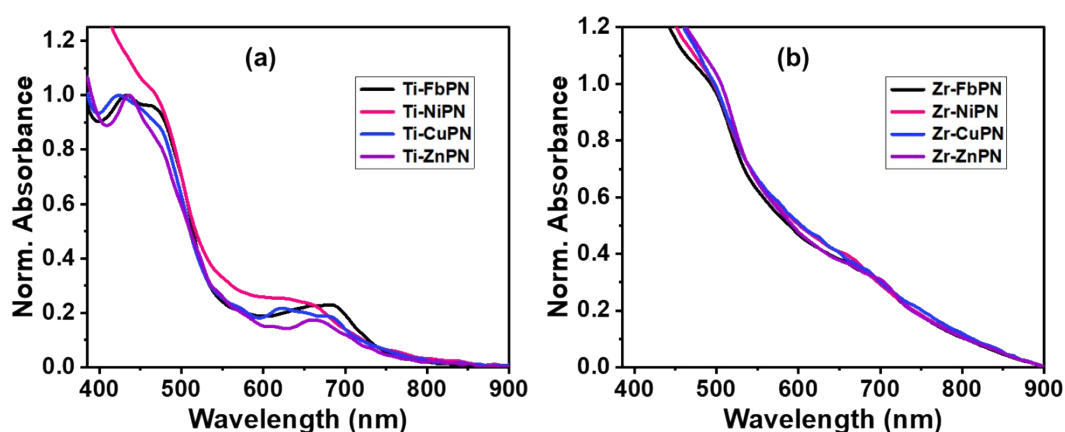


Fig. S2 Normalized absorbance of PN's monolayer (a) on TiO₂ films, (b) on ZrO₂ films.

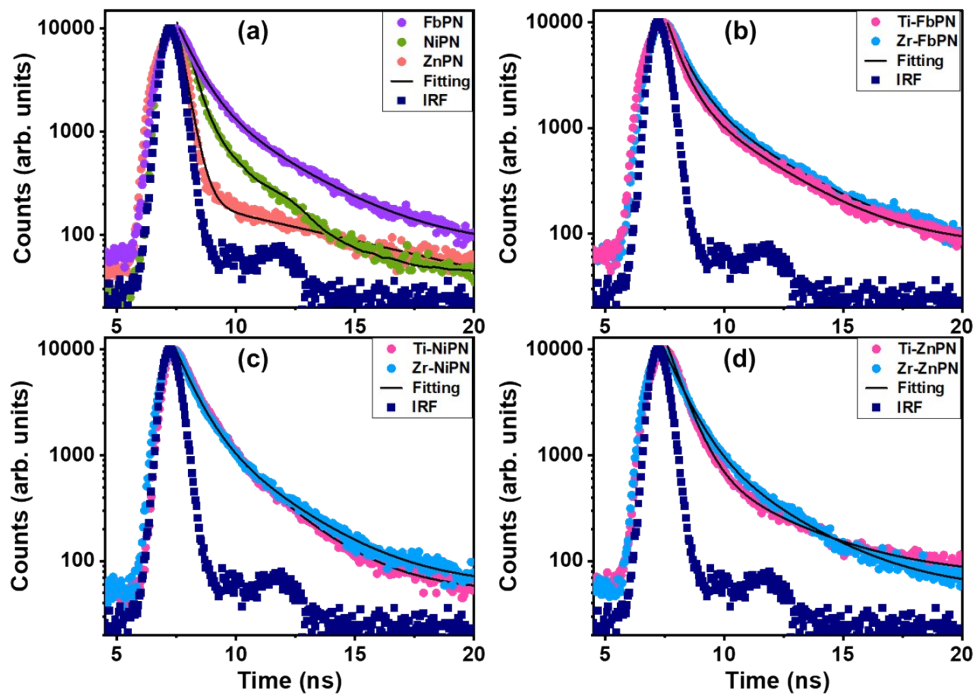


Fig. S3 (a) Time-resolved photoluminescence (TRPL) of PN films; TRPL of (b) free-base (Fb), (c) Ni and (d) Zn-porphyrin-naphthalimide adsorbed on TiO₂ and ZrO₂.

Table S1 TRPL data fitting results and average lifetimes (Ave. lifetime).

Sample	$\tau_1(ns)$	Rel. %	$\tau_2(ns)$	Rel. %	Ave. lifetime (ns)	χ^2
FbPN	0.52	68.67	8.63	31.33	2.31	1.46
NiPN	0.41	72.09	3.79	27.91	1.86	1.42
ZnPN	0.33	74.72	4.22	25.28	1.23	1.33
Ti-FbPN	0.55	45.52	3.71	54.48	2.54	1.50
Zr-FbPN	0.72	48.09	3.80	51.91	2.55	1.41
Ti-NiPN	0.73	55.42	2.13	44.58	1.29	1.39
Zr-NiPN	0.72	50.14	2.51	49.86	1.67	1.29
Ti-ZnPN	0.69	63.19	2.71	36.81	1.46	1.46
Zr-ZnPN	0.82	71.69	2.69	28.31	1.63	1.35

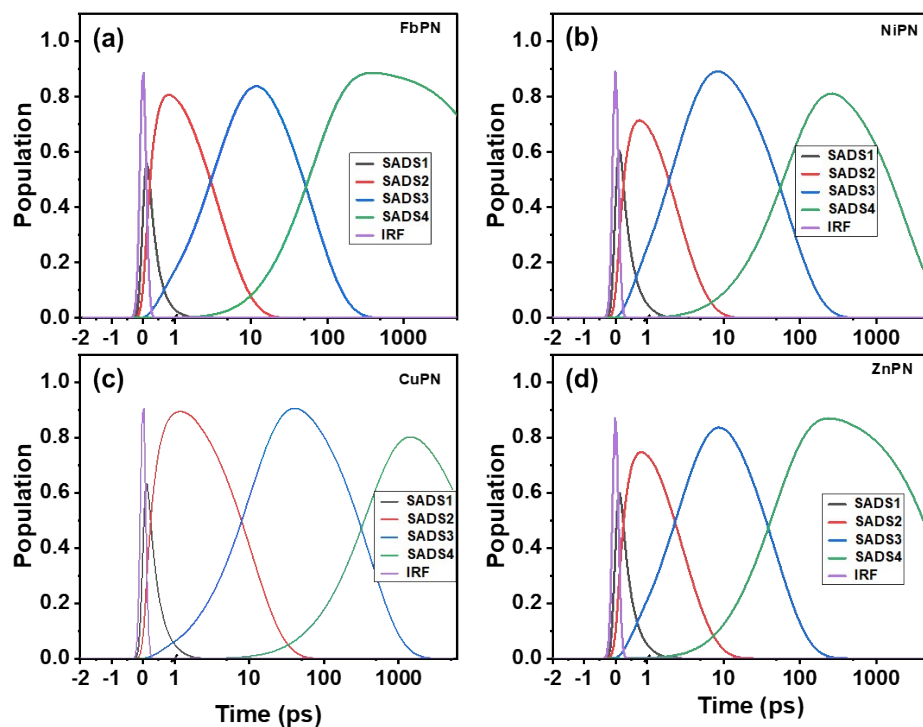


Fig. S4 (a), (b), (c), and (d)- population decay profiles of the respective species associated difference spectra (SADS) obtained from target analysis of TAS data for FbPN, NiPN, CuPN and ZnPN, respectively.

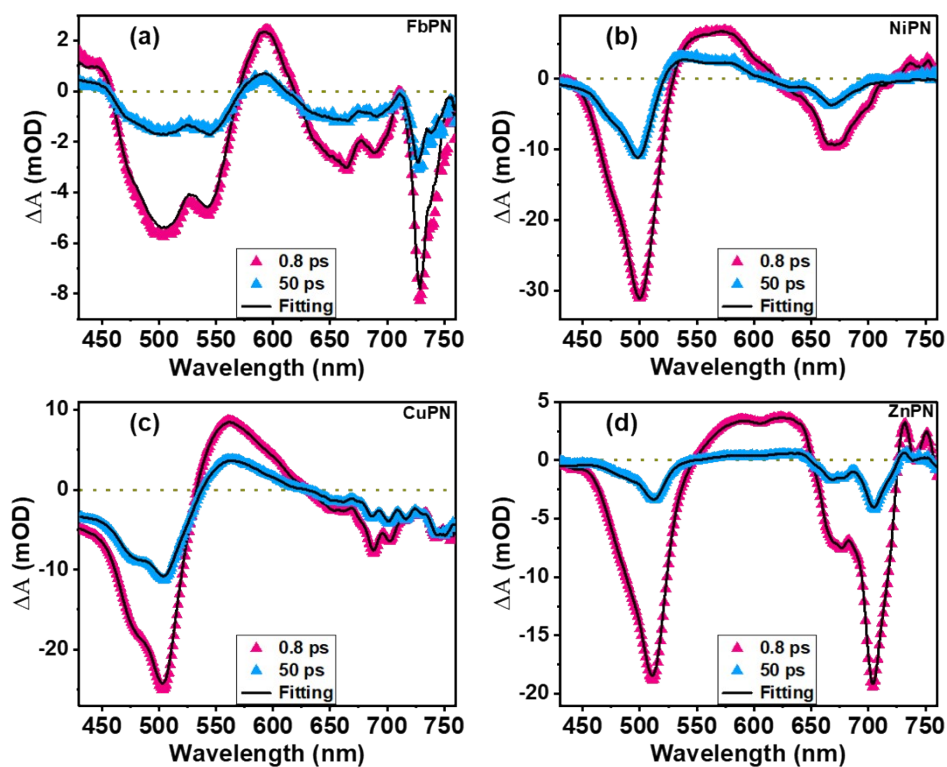


Fig. S5 Kinetic trace fittings for the delay time of 0.8 and 50 ps from the target model analysis of (a)FbPN, (b)NiPN, (c)CuPN and (d)ZnPN. Open symbols are experimental data and solid black lines are fittings.

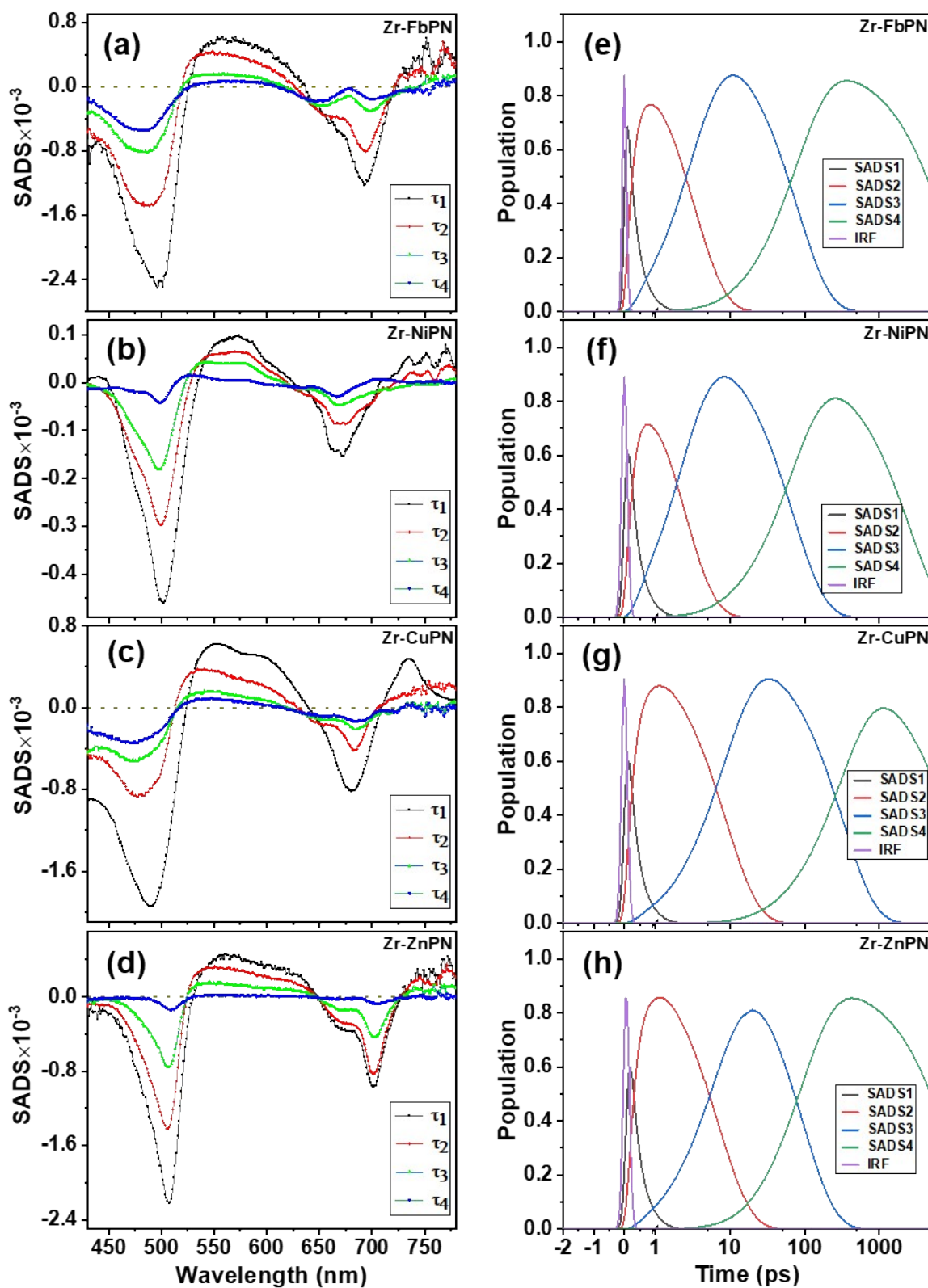


Fig. S6 (a), (b), (c), and (d)- species associated difference spectra (SADS) obtained from target analysis of TAS data for Zr-FbPN, Zr-NiPN, Zr-CuPN and Zr-ZnPN, respectively; (e), (f), (g), and (h) population decay profiles of the respective SADS.

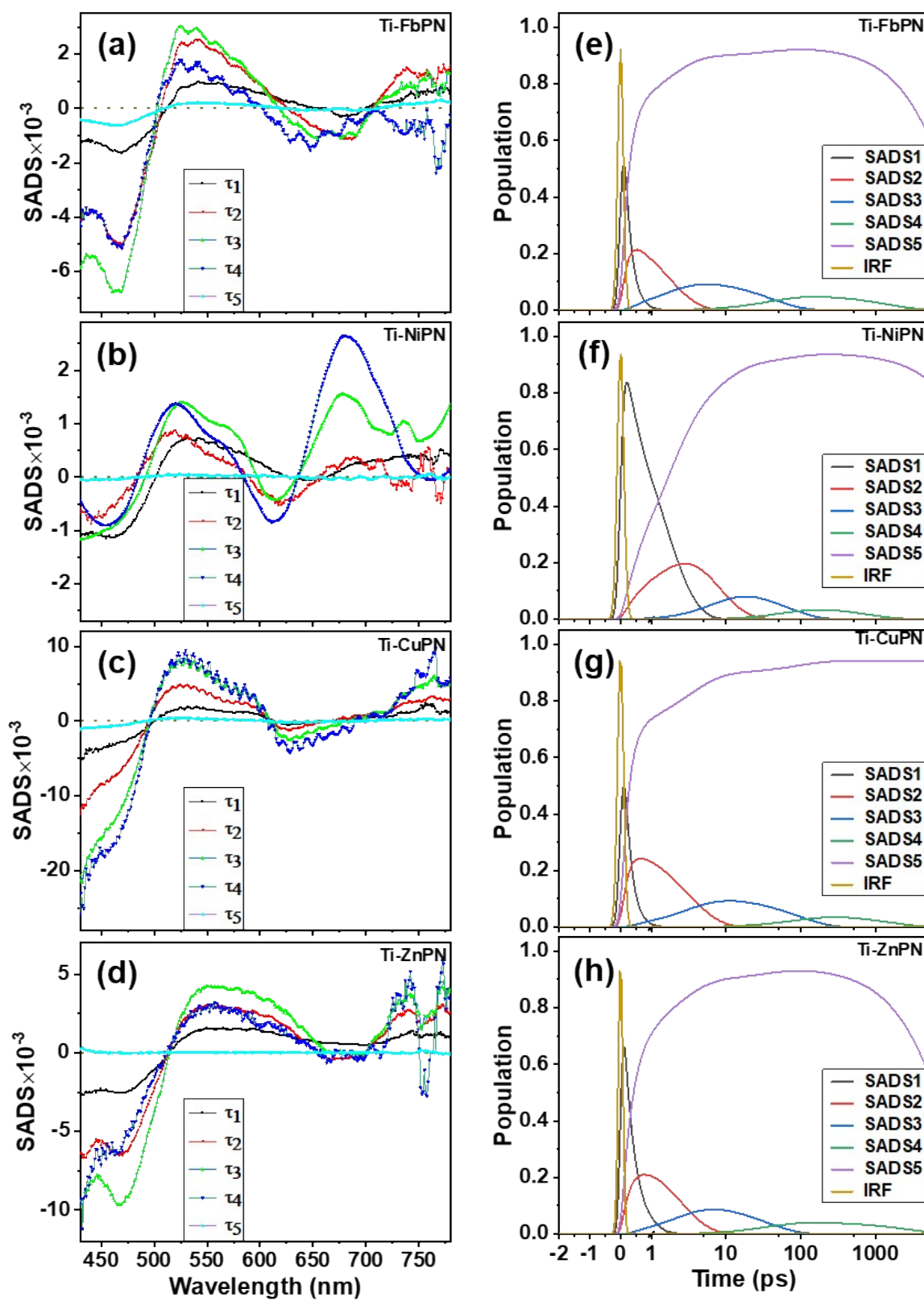


Fig. S7 (a), (b), (c), and (d)- species associated difference spectra (SADS) obtained from target analysis of TAS data for Ti-FbPN, Ti-NiPN, Ti-CuPN and Ti-ZnPN, respectively; (e), (f), (g), and (h) population decay profiles of the respective SADS.

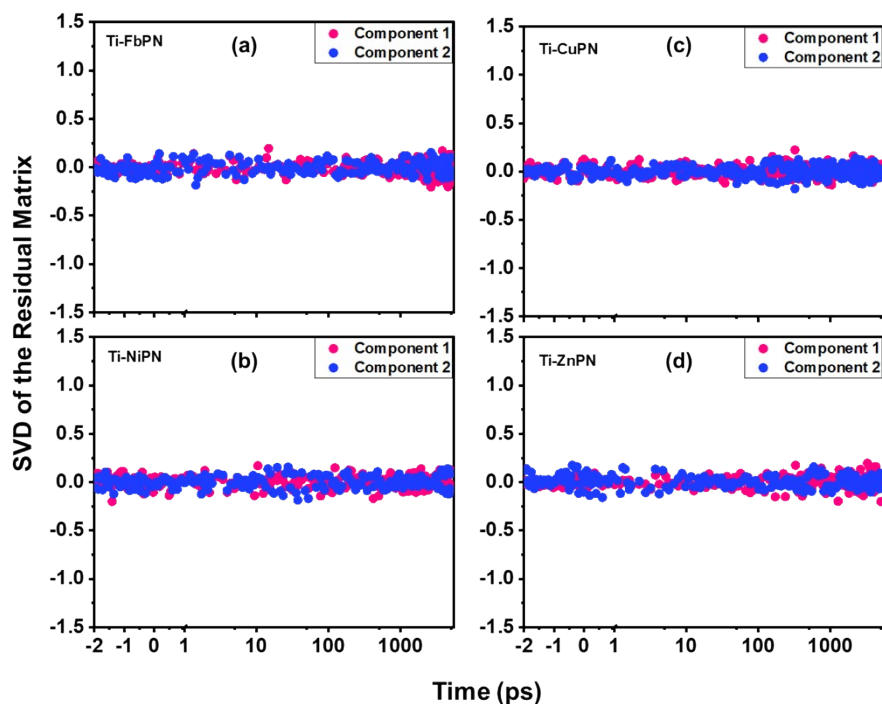


Fig. S8 Singular value decomposition (SVD) of the residual matrix after target analysis of TAS data for (a) Ti-FbPN, (b) Ti-NiPN, (c) Ti-CuPN, (d) Ti-ZnPN.

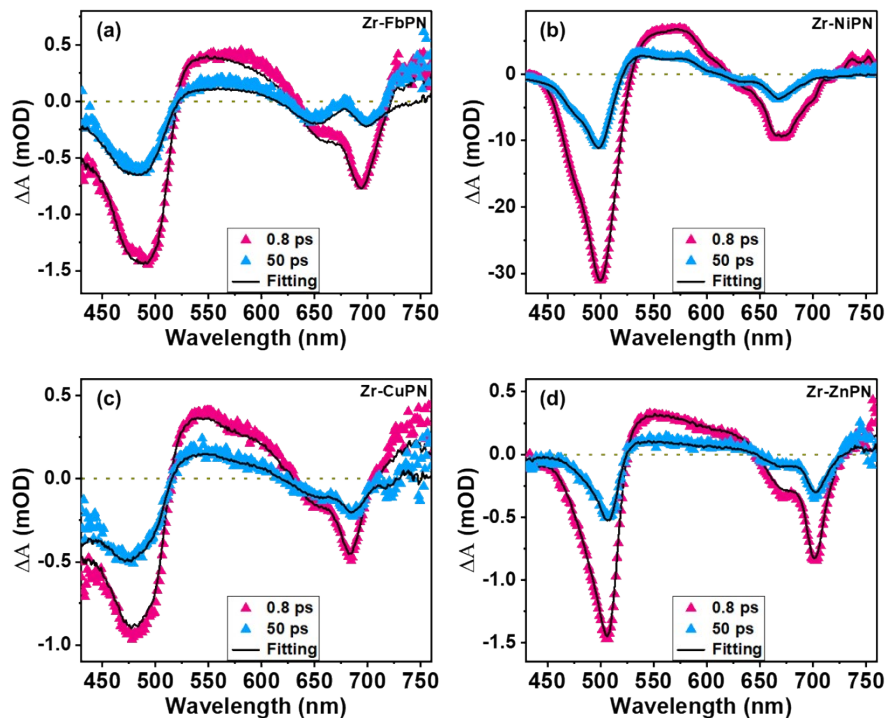


Fig. S9 (a), (b), (c), and (d)- fs-TAS at probe delay of 0.8 and 50 ns, for Zr-FbPN, Zr-NiPN, Zr-CuPN and Zr-ZnPN, respectively. Experimental data are represented by scattered symbols, whereas solid lines represent target analysis fittings.

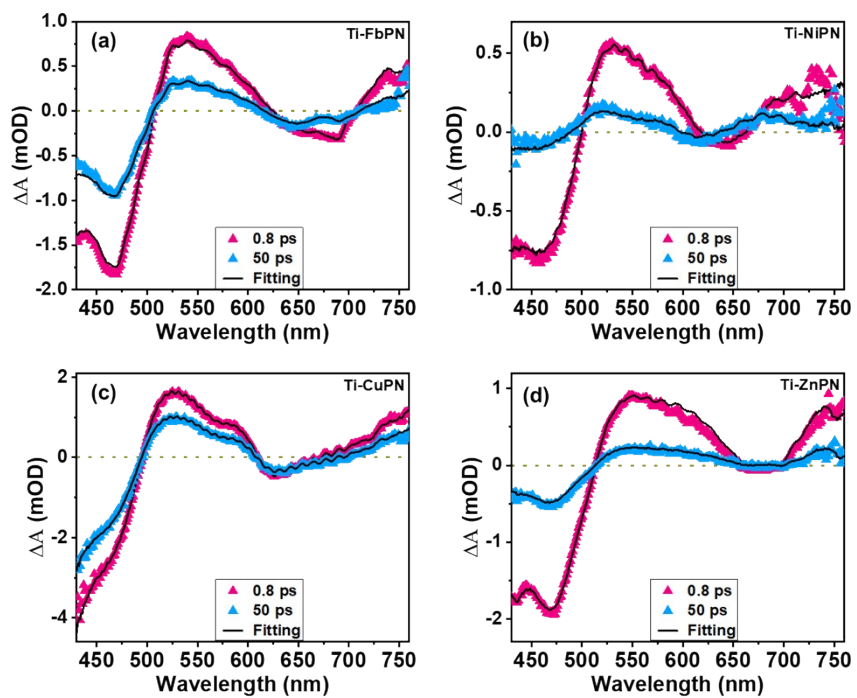


Fig. S10 (a), (b), (c), and (d)- fs-TAS at probe delay of 0.8 and 50 ns, for Ti-FbPN, Ti-NiPN, Ti-CuPN and Ti-ZnPN, respectively. Experimental data are represented by scattered symbols, whereas solid lines represent target analysis fittings.